Thermal equation of state for Pt

Shikai Xiang,* Lingcang Cai, Yan Bi, and Fuqian Jing
Laboratory for Shock Wave and Detonation Physics Research, Institute of Fluid Physics, P.O. Box 919-102, 621900 Mianyang, Sichuan, People's Republic of China

Shunjin Wang
College of Physical Science and Technology, Sichuan University, 610064 Chengdu, People's Republic of China
(Received 24 July 2005; revised manuscript received 30 September 2005; published 15 November 2005)

The thermal equation of state of fcc platinum has been evaluated by using the full-potential linear muffin-tin orbital (FPLMTO) total-energy method combined with a mean-field model of the vibrational partition function for pressures up to 1000 GPa and temperatures up to 10 000 K. The equation of state at zero temperature was computed using FPLMTO. For the finite temperatures, the vibrational contributions were obtained by computing the partition function using the particle in a cell model in the mean field which was constructed from the sum of all the pair potentials between the reference atom and the others of the system. The calculated properties are in good agreement with available static and shock-wave experimental measurements.

DOI: 10.1103/PhysRevB.72.184102 PACS number(s): 64.30.+t, 05.70.Ce, 71.20.Be, 65.20.+w

I. INTRODUCTION

Platinum is an important pressure standard owing to its chemical inertness, large isothermal compressibility, and the large pressure and temperature stability ranges of its ambient face-centered-cubic (fcc) phase. In addition, platinum's ability to absorb infrared radiation makes it a commonly used laser absorber and internal pressure standard in laser heated diamond cell experiments designed to measure high pressure high-temperature phase stability and equations of state (EOS). As one of the best pressure scales, the EOS of platinum has been studied to 660 GPa with a two-stage light gas gun and by a non-full-potential-based first principles theoretical treatment[1] combined with some approximation such as the atomic-sphere approximation[2] and the approximate ion Grüneisen parameter form due to Slater.[3] The elasticity and rheology of platinum under high pressure and nonhydrostatic stress has also been investigated recently.[4] Despite the high quality of the experimental Hugoniot of the platinum, qualifying it as an ultrahigh-pressure standard for dynamic experiments, improved accuracy of the isotherm is also needed to qualify it as a pressure standard for static experiments, especially at high temperature.

First principles electronic structure methods are routinely used to compute the zero-temperature internal energy, but also can be used to calculate the Helmholtz free energy contributions from the ions and electrons. They result in a complete equation of state from which properties such as thermal expansion coefficients, bulk moduli, specific heat, and thermal Grüneisen parameter of the system can be deduced. The smaller Helmholtz free energy contribution from the electrons usually can be calculated using the finite temperature density functional approach of Mermin.[5] However, the contribution from the ions is difficult to calculate accurately because the volume and temperature dependence of the phonon frequencies and the density of states are complicated. One of the most accurate methods for handling this problem, especially at high temperatures (above the Debye temperature and below melt), is the particle-in-a-cell (PIC) model.[6,7] The advantage of the PIC model over lattice dynamics based on the quasiharmonic approximation is that the anharmonic contributions from the potential energy of the system are included exactly without a perturbation expansion. The PIC model is essentially an anharmonic Einstein model, and the $3N$-dimensional partition function is reduced to a simple three-dimensional integral.[8] Calculations using this model usually are performed on supercells of several hundreds of atoms for each lattice with periodic boundary conditions. The PIC model has been demonstrated to match successfully the thermal properties of iron,[9] aluminum,[10] and copper[11] as well as the the high-pressure thermoelasticity[8] and thermal equation of state[12] of body-centered-cubic tantalum.

In this investigation the isotherms of fcc platinum at different temperatures have been calculated using a full-potential linear muffin-tin orbital (FPLMTO) total-energy method[13] combined with a pair-potential-based mean-field approximation (PPBMFA)[10] to the thermal contribution to the Helmholtz free energy based on the PIC model.

II. COMPUTATIONAL METHODS FOR HELMHOLTZ FREE ENERGY

For a system with a given averaged atomic volume V and temperature T, the Helmholtz free energy $F(V,T)$ per ion can be separated as

$$F(V,T) = E_0(V) + F_{\mathrm{el}}(V,T) + F_{\mathrm{ion}}(V,T), \tag{1}$$

where $E_0(V)$ is the static zero temperature energy, $F_{\mathrm{el}}(V,T)$ is the electronic contribution, and $F_{\mathrm{ion}}(V,T)$ is the vibrational contribution. The first two terms on the right-hand side can be calculated using density functional theory (DFT) generalized to finite temperatures by the Mermin theorem.[5]

Above the Debye temperature, in the PIC model $F_{\mathrm{ion}}(V,T)$ can be expressed approximately as[6,7]

$$F_{\text{ion}} = -k_B T \ln\left[\left(\frac{mk_B T}{2\pi\hbar^2}\right)^{3/2} f(V,T)\right], \tag{2}$$

where

$$f(V,T) = \int_{\text{WS}} dr \exp[-(U(\mathbf{r}) - U_0)/k_B T], \tag{3}$$

$\hbar$ and k_B are Planck's constant and Boltzmann's constant, respectively, m is the mass of each ion, U_0 is the potential energy of the system with all ions on ideal lattice sites, and $U(\mathbf{r})$ is the potential energy of the system with the wanderer ion displaced by the radius vector $\mathbf{r}$ from its equilibrium position. The key problem for calculating F_{ion} is to determine the change of potential energy of the system due to the displacement of the wanderer ion and to perform the integration over the Wigner-Seitz cell.

In the conventional PIC model the potential energy $U(\mathbf{r})$ is calculated on supercells of several dozens or hundreds of atoms (usually $N=32-108$) for each lattice with periodic boundary conditions using mixed basis pseudopotential methods[12] or a tight-binding total-energy method,[8,9] whereas using the PPBMFA[10] $U(\mathbf{r})$ can be directly constructed according to the symmetry of lattice from the pair potential ϕ, which in turn can be obtained from its relationship with the total energy of the single-atom unit cell

$$E(a) = \frac{1}{2}\sum_{\mathbf{R}} \phi(\|\mathbf{R}\|), \tag{4}$$

where a is the lattice constant, $\mathbf{R}$ denotes the lattice vectors of all ions in the system except the wanderer ion, and the site of the wanderer ion is the zero lattice vector.

In order to obtain the pair potential accurately, we divided the system into two zones using a sphere of radius R_{cut} centered on the equilibrium position of the reference atom. In the zone of $\|\mathbf{R}\| > R_{\text{cut}}$ the sum of pair potential over $\mathbf{R}$ was replaced by the integral

$$\sum_{\|\mathbf{R}\|>R_{\text{cut}}} \phi(\|\mathbf{R}\|) = \int_{\infty}^{R_{\text{cut}}} 4\pi l^2 \rho(a)\phi(l)dl, \tag{5}$$

where ρ denotes the number of ions per unit volume (for fcc Pt $\rho = 4/a^3$) and l is the distance between two ions. The pair potential was assumed to be of the form

$$\phi(l) = -xl^m + yl^n, \tag{6}$$

where x and y are positive constants and m and n are negative constants. Using these approximations, Eq. (4) was rewritten as

$$E(a) = \frac{1}{2}\sum_{\|\mathbf{R}\|\le R_{\text{cut}}} \phi(\|\mathbf{R}\|) - \frac{8\pi}{a^3}\left(\frac{x}{m+3}R_{\text{cut}}^{m+3} - \frac{y}{n+3}R_{\text{cut}}^{n+3}\right). \tag{7}$$

After a cutoff radius test, R_{cut} was set to a fixed value. The four parameters x, y, m, and n in the pair potential then were evaluated by fitting the results for the static total energies $E(a)$ versus lattice constant to Eq. (7).

Using this pair potential and the same R_{cut}, the potential energy difference $U(\mathbf{r}) - U_0$ in Eq. (3) was calculated using the approximation

$$U(\mathbf{r}) - U_0 = \frac{1}{2}\sum_{\mathbf{R}\le R_{\text{cut}}} \phi(\|\mathbf{R}-\mathbf{r}\|) - \frac{1}{2}\sum_{\mathbf{R}\le R_{\text{cut}}} \phi(\|\mathbf{R}\|). \tag{8}$$

The integration in Eq. (3) was replaced approximately by a weighted sum of a small number of special points in the irreducible zone of Wigner-Seitz cell. Here we used a uniform grid of $\mathbf{r}$ points which is analogous to the Monkhorst-Pack grid[14] in reciprocal space.

III. EQUATION OF STATE

A. Static equation of state

The static zero-temperature high-pressure properties of Pt were obtained from first principles by using the FPLMTO total-energy method.[13] The $6s$, $6p$, and $5d$ states were treated as valence states, the $5p$ states as semicore states and the others as core electrons. We used both the local density approximation (LDA)[15] and the generalized gradient approximation (GGA)[16] for the exchange-correlation potential. Three sets (triple-k basis[17]) of LMTO envelopes were used, and in each channel s-, p-, d-, and f-partial waves were included. All calculations reported here used an $18\times18\times18$ k-point mesh after convergence tests. Spin-orbit interactions were found to have only a negligible effect on the equation of state, so our computations were done without spin-orbit coupling for the valence states and semicore states. The core states were fully relativistic.

In order to obtain the static pressure accurately we computed the total energy for 67 different atomic volumes ranging from 8.01 to 16.64 Å^3, and the energies were fit to the Vinet equation[18] and the fourth-order Birch equation of state,[19] respectively. Pressures were obtained analytically from the derivatives. The differences of GGA pressures from the Vinet fit and the fourth-order Birch fit (Fig. 1) are negligible. Similarly, the differences of the LDA pressure from the Vinet fit and the fourth-order Birch fit are also negligible. So all the results below were obtained from the Vinet fit.

The zero-pressure properties of the Vinet fit are shown in Table I. These results are consistent with the general expectation that the LDA and GGA models will produce volumes that bound the experimental value. The LDA and GGA bulk moduli found here also bracket the measured room temperature value, with the LDA value being 8% larger and the GGA value being 12% smaller. All of these zero-pressure results show that the LDA model yields rather good agreement with the existing zero-pressure data and is clearly preferable to the GGA model for determining the low pressure EOS of this particular material.

Because the pressure contribution from the electron excitations and lattice vibrations at ambient temperature is small, the calculated equation of state at zero temperature is compared directly with room-temperature data in Fig. 2. The LDA results are also found to be more accurate than the GGA. All these results serve as a reminder again that there are a number of systems, such as Au,[23] Ta,[12] and Pt, for

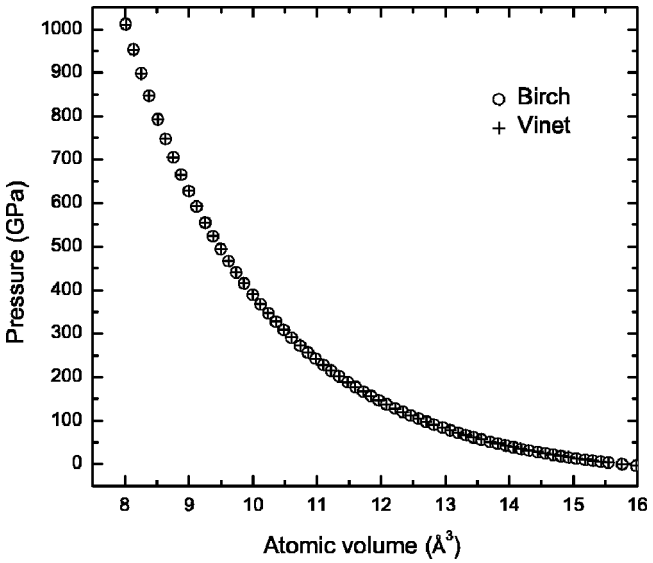

FIG. 1. Comparison of GGA pressure from different equations of state, the Vinet equation (Ref. 18) and the fourth-order Birch equation of state (Ref. 19).

which the LDA model works better than the presumably more advanced GGA model. Based on the above analysis, LDA also should provide more reliable results at high temperature than GGA does. So all the thermal properties below were calculated using LDA.

B. Thermal equation of state

We divided the pressure at a certain high temperature and volume into two parts, one is from the $E_0(V)$ and $F_{\mathrm{el}}(V,T)$, which were obtained using a self-consistent electronic structure calculation generalized to a finite temperature by Mermin theorem,[5] and the other is from $F_{\mathrm{ion}}(V,T)$, which was calculated using the improved PPBMFA method as described above. The details of the self-consistent electronic structure calculation are the same as the case at zero temperature except for thermal contributions. The total energy $E(V,T)$ from electronic structure calculation was fit to the Vinet equation and the pressure was obtained analytically from

TABLE I. Theoretical static-lattice, zero-temperature zero-pressure atomic volumes (V_0), bulk moduli (K_0), and pressure derivatives of the bulk moduli (K_0') obtained here for fcc Pt using the LDA and GGA models without spin-orbit coupling, are compared to previous LMTO calculations and experiments at 300 K.

	V_0 (Å^3/atom)	K_0 (GPa)	K_0'
LDA	14.90	300.9	5.814
GGA	15.77	243.3	5.866
LMTO		266[a]	5.81[a]
Experiments	15.06[b]	278[b]	5.61[c]

[a]From Ref. 1.
[b]From Ref. 20.
[c]From Ref. 21.

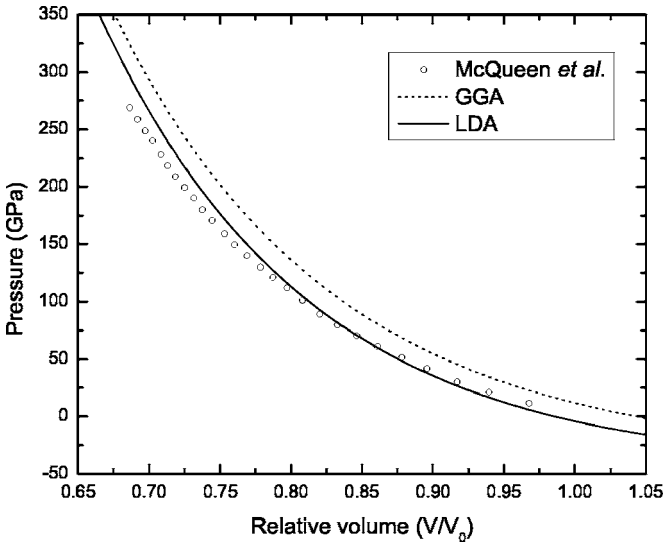

FIG. 2. Static equation of state of Pt. Solid and dashed lines are LDA and GGA calculations, respectively. Circles are the shock-reduced 300 K isotherm of McQueen *et al.* (Ref. 22). Volumes are given relative to the experimental room temperature volume, 15.06 Å^3.

$$P_1 = 3K_0(1-z)z^2 \exp[(1.5K_0' - 1.5)(1-z)], \qquad (9)$$

where $z=(V/V_0)^{1/3}$. The fit parameters are given in Table II.

In order to obtain the vibrational contributions to the free energy accurately, we used 33 additional LDA-energy data with different atomic volumes ranging from 16.64–20.96 Å^3 in addition to the data for the 67 different atomic volumes ranging from 8.01 to 16.64 Å^3 at each temperature to fit the parameters in the pair potential. The temperatures (besides 300 K) range from 1000 to 10 000 K in steps of 1000 K. After a cutoff radius test, we found that it was accurate enough to set $R_{\mathrm{cut}}=6a$, which produced 3588 nearest ions from the wanderer ion within the sphere, to evaluate the pair potential. The pair potential is not sensitive to increasing temperature even at 10 000 K and the temperature depen-

TABLE II. Fitted Vinet EOS parameters for the LDA energy at different temperatures.

T (K)	E_0 (eV)	V_0 (Å^3/atom)	K_0 (GPa)	K_0'
0	−501841.07367	14.90	300.9	5.814
300	−501841.07149	14.90	301.1	5.813
1000	−501841.05421	14.89	302.2	5.810
2000	−501841.01511	14.88	303.0	5.811
3000	−501840.96658	14.87	303.2	5.817
4000	−501840.90928	14.84	306.7	5.796
5000	−501840.84022	14.81	310.7	5.780
6000	−501840.75833	14.76	316.3	5.757
7000	−501840.66210	14.70	324.0	5.726
8000	−501840.55111	14.63	333.8	5.687
9000	−501840.42433	14.54	345.4	5.642
10000	−501840.28162	14.45	358.6	5.595

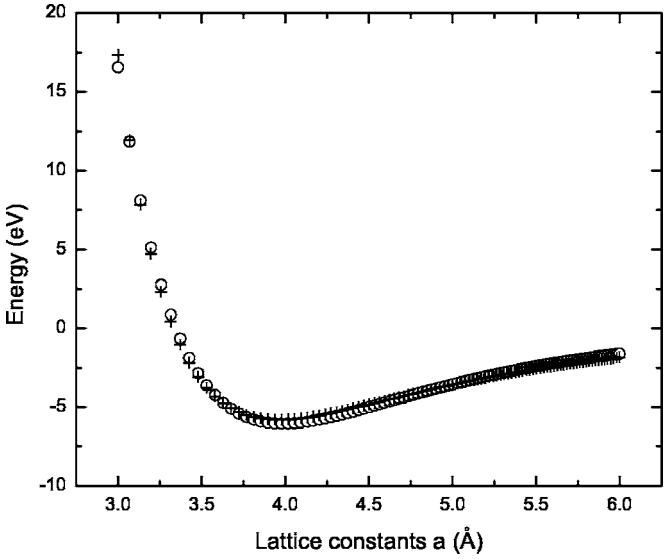

FIG. 3. Comparison of the energy from the LDA calculations (circles) and from the superposition of the pair potential (crosses) with the fitted parameters.

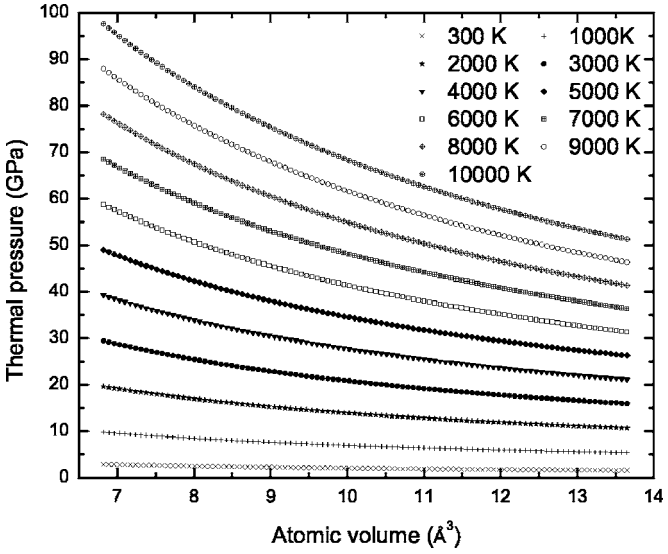

FIG. 4. Thermal pressure from the ion vibrational contribution as a function of volume at different temperatures.

dence of potential energy difference $U(\mathbf{r})-U_0$ in Eq. (8) is negligible. So the zero-temperature pair potential was used to calculate the potential energy difference for all the different temperatures. The fit values of x, y, m, and n for the zero-temperature pair potential $\phi(l)=-xl^m+yl^n$ are 760, 2513, −5.1572, and −6.3574, respectively and the parameters of the fit are given in units which gives energy in eV and l in Å. The quality of the fit is shown in Fig. 3. A uniform $200\times200\times200$ **r**-point grid, which is analogous to the Monkhorst-Pack grid[14] in reciprocal space, was used to perform the integration in Eq. (3) for F_{ion}. At each temperature 100 values of F_{ion} with different atomic volumes ranging from 6.82 to 13.65 Å^3 were calculated and fit to a fourth-order polynomial in volume. Then the thermal pressures from the vibrational contribution were obtained directly from the negative volume derivative of the polynomial. The thermal pressures (Fig. 4) at a certain high temperature clearly increase with decreasing volume. It should be mentioned here that all our results make sense only at temperatures below the melting point at certain high pressure. (At ambient pressure the melting temperature is 2041.4 K.) For anticipated further use of our thermal pressure data, we present the analytic representation of the pressure as the function of relative volume X ($X=V/V_0$),

$$P_2 = A_0 + A_1X + A_2X^2 + A_3X^3 + A_4X^4, \qquad (10)$$

and the values of corresponding parameters A_0, A_1, A_2, A_3, and A_4 (Table III), obtained from the negative volume derivative of vibrational free energy. The parameters shown in Table III are given in units which give pressure in GPa.

The sum of static pressure in Eq. (9) and thermal pressure in Eq. (10) volume gives the the isotherms in Fig. 5. As a comparison, the zero-temperature isotherm was also included in Fig. 5. We compare our isotherm at high temperatures with the theoretical results of Holmes *et al.*[1] (dotted lines) in Fig. 6. Our results are slightly stiffer than theirs. The calculated 300 K isotherm is also compared with the theoretical results of Holmes *et al.*[1] and the shock-reduced results of McQueen *et al.*[22] in Fig. 7. Similarly our results are slightly stiffer than theirs above 100 GPa. The main reason why our isotherms are stiffer may be that our full-potential-based total-energy calculations[13] are more sensitive to the compression than the total-energy calculations using the atomic-sphere approximation[2] used by them. The full-potential-based total-energy calculations without using the atomic-sphere approximation, in principle, is more accurate. Furthermore, we calculated the thermal properties without using the approximate ion Grüneisen parameter γ_{ion} form due to Slater,[3] used by Holmes *et al.*,[1] or the assumption $\gamma_{\text{ion}}=2.4(V/V_0)$ and electron-Grüneisen parameter $\gamma_{\text{el}}=0$, used by McQueen *et al.*[22] For these reasons, our results should be more reliable, especially the 300 K isotherm.

To compare our results of the equation of state of Pt at high compression and high temperatures with those derived

TABLE III. Parameters for analytic representation of the pressure in Eq. (10) at different temperatures. The parameters are given in units which give pressure in GPa.

T (K)	A_0	A_1	A_2	A_3	A_4
300	9.7111	−28.8801	43.5109	−32.2936	9.4902
1000	32.7523	−98.4956	149.8067	−112.1764	33.2013
2000	65.5072	−197.0213	299.5981	−224.4228	66.3977
3000	98.2672	−295.5985	449.4428	−336.8440	99.6675
4000	131.0293	−394.2061	599.2904	−449.3934	133.0137
5000	163.7891	−492.8144	749.0622	−561.9815	166.4126
6000	196.5434	−591.3976	898.6856	−674.5177	199.8342
7000	229.2898	−689.9375	1048.1053	−786.9264	233.2507
8000	262.0271	−788.4240	1197.2854	−899.1518	266.6400
9000	294.7555	−886.8540	1346.2088	−1011.1579	299.9860
10000	327.4756	−985.2308	1494.8741	−1122.9262	333.2791

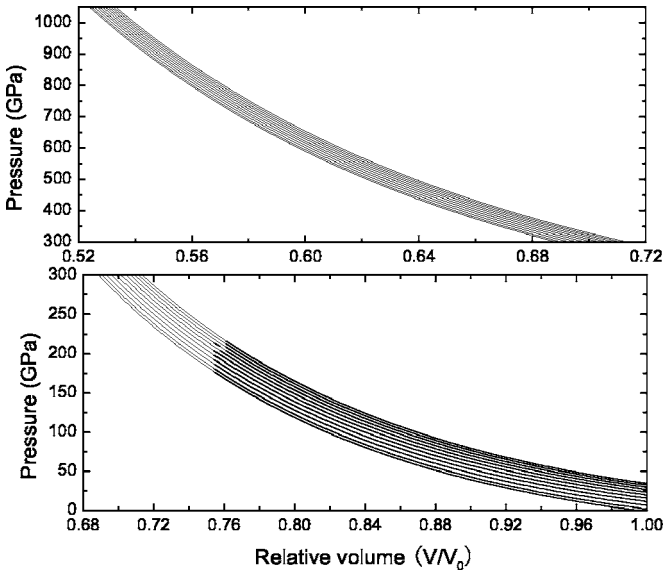

FIG. 5. Theoretical isotherms for platinum at different temperatures. The curves correspond (from bottom to top) to temperatures from 0 to 10 000 K in steps of 1000 K. Volumes are given relative to the experimental room temperature volume, 15.06 Å^3.

from the shock data, we also calculated the pressures P_H and temperatures T_H on the Hugoniot for a set of relative volumes ranging from 0.925 to 0.675 by solving the Rankine-Hugoniot equation[24]

$$P_H(V_0 - V) = 2(E_H - E_0), \tag{11}$$

where E_H is internal energy along the Hugoniot, and E_0 and V_0 are, respectively, zero-pressure room-temperature energy and volume of the FPLMTO results. For a given volume V, the temperature on the Hugoniot is varied until Eq. (11) is satisfied. The agreement of the calculated Hugoniot with experimental data[1,22] is excellent in Fig. 8.

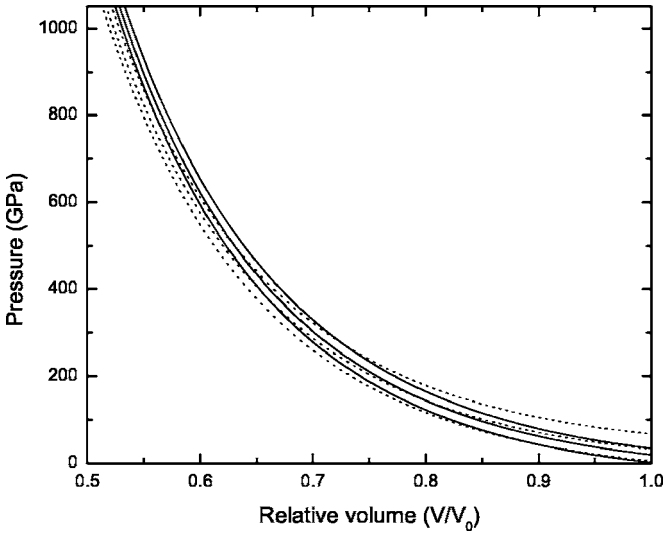

FIG. 6. Our theoretical isotherms (solid lines) for platinum at high temperatures as compared against the theoretical results of Holmes *et al.* (Ref. 1) (dotted lines). Both the solid lines and the dotted lines correspond (from bottom to top) to 1000 K, 5000 K, and 10 000 K, respectively. Volumes are given relative to the experimental room temperature volume, 15.06 Å^3.

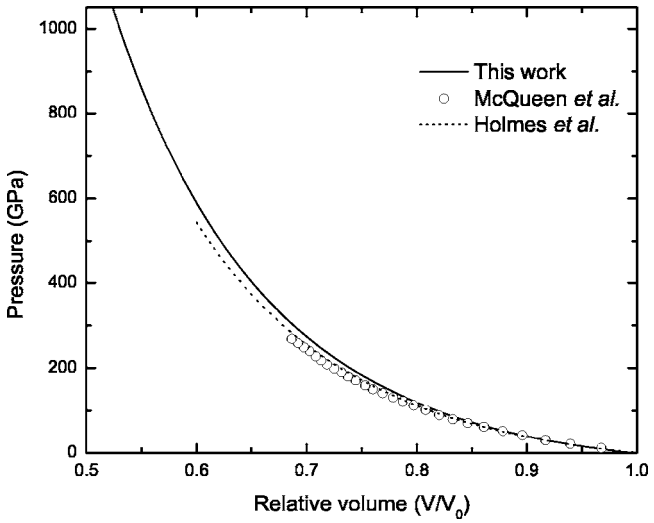

FIG. 7. Theoretical 300 K isotherms for platinum as compared to the shock-reduced 300 K isotherm of McQueen *et al.* (Ref. 22) and the theoretical results of of Holmes *et al.* (Ref. 1). Volumes are given relative to the experimental room temperature volume, 15.06 Å^3.

IV. SUMMARY

The equation of state of platinum has been calculated to pressures up to 1000 GPa and temperatures up to 10 000 K, with and without spin-orbit coupling effects included, using

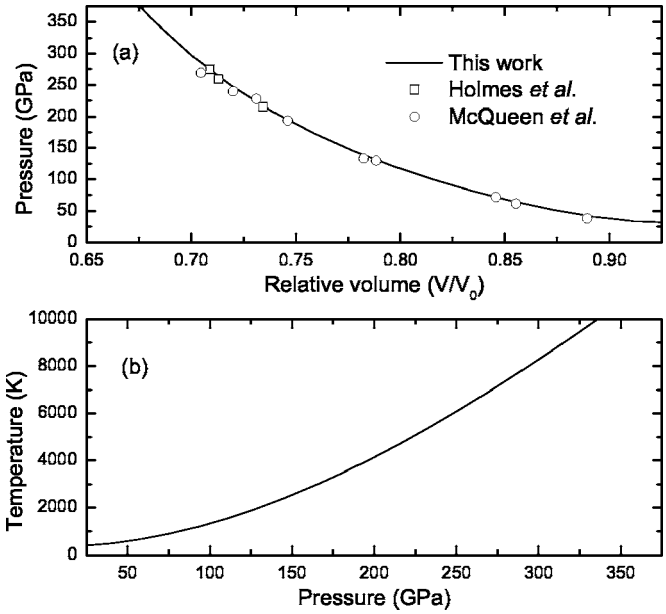

FIG. 8. (a) Theoretical Hugoniot for platinum compared to experimental Hugoniot data of Holmes *et al.*[1] and McQueen *et al.*[22] Volumes are given relative to the experimental room temperature volume, 15.06 Å^3. (b) Theoretical temperatures along the Hugoniot.

LDA and GGA. It is shown that spin-orbit coupling effects are negligible, while density gradient corrections are significant. Once thermal effects are accounted for, the LDA model produces a room temperature isotherm that is in reasonably better agreement with existing data than the GGA model does. So the LDA zero temperature isotherm was used as a starting point for obtaining its counterparts at high temperatures. The pair potential, which was used to construct the mean field and to compute the vibrational partition function, has a negligible temperature dependence. The calculated Hugoniot is in excellent agreement with available shock-wave experimental measurements, but the calculated isotherms are slightly stiffer than the previous LMTO results[1] with the atomic-sphere approximation[2] and the ion Grüneisen parameter γ_{ion} form due to Slater.[3]

ACKNOWLEDGMENTS

This work was supported by the National Science Foundation of China (Grant No. 10299040). The authors are grateful to D. Yu Savrasov and S. Yu Savrasov for providing their LMTART code. The authors thank Jian Xu for helpful discussions.

*Electronic address: xiangshikai@yahoo.com

[1] N. C. Holmes, J. A. Moriarty, G. R. Gathers, and W. J. Nellis, J. Appl. Phys. **66**, 2962 (1989).
[2] H. L. Skriver, *The LMTO Method* (Springer, Berlin, 1984).
[3] J. C. Slater, *Introduction to Chemical Physics* (McGraw-Hill, New York, 1939).
[4] A. Kavner and T. S. Duffy, Phys. Rev. B **68**, 144101 (2003).
[5] N. D. Mermin, Phys. Rev. **137**, A1441 (1965).
[6] A. C. Holt and M. Ross, Phys. Rev. B **1**, 2700 (1970).
[7] K. Westera and E. R. Cowley, Phys. Rev. B **11**, 4008 (1975).
[8] O. Güseren and R. E. Cohen, Phys. Rev. B **65**, 064103 (2002).
[9] E. Wasserman, L. Stixrude, and R. E. Cohen, Phys. Rev. B **53**, 8296 (1996).
[10] S. Xiang, L. Cai, F. Jing, and S. Wang, Phys. Rev. B **70**, 174102 (2004).
[11] S. Xiang, L. Cai, F. Jing, and S. Wang, Chin. Phys. Lett. **22**, 424 (2005).
[12] R. E. Cohen and O. Güseren, Phys. Rev. B **63**, 224101 (2001).
[13] S. Y. Savrasov and D. Y. Savrasov, Phys. Rev. B **46**, 12181 (1992).
[14] H. J. Monkhorst and J. D. Pack, Phys. Rev. B **13**, 5188 (1976).
[15] S. H. Vosko, L. Wilk, and M. Nusair, Can. J. Phys. **58**, 1200 (1980).
[16] J. P. Perdew, K. Burke, and M. Ernzerhof, Phys. Rev. Lett. **77**, 3865 (1996).
[17] M. Methfessel, Phys. Rev. B **38**, 1537 (1988).
[18] P. Vinet, J. H. Rose, J. Ferrante, and J. R. Smith, J. Phys. C **1**, 1941 (1987).
[19] F. Birch, J. Geophys. Res. B **83**, 1257 (1978).
[20] C. Kittel, *Introduction to Solid State Physics* (Wiley, New York, 1996).
[21] D. J. Steingerg, J. Phys. Chem. Solids **43**, 1173 (1982).
[22] R. G. McQueen, S. P. Marsh, J. W. Taylor, J. N. Fritz, and W. J. Carter, in *High-Velocity Impact Phenomena*, edited by P. Kinslow (Academic, New York, 1970).
[23] J. C. Boettger, Phys. Rev. B **67**, 174107 (2003).
[24] M. A. Meyers, *Dynamic Behavior of Materials* (Wiley, New York, 1994).